

# Transfer of Technologies for Performance Degradation Prediction and Channel Switching in Vehicular Networks under Harsh Weather Conditions and Integration with State-of-the-Art Products

Final Report

By

**Dr. Chin-Tser Huang**, University of South Carolina  
**Dr. Gurcan Comert**, North Carolina A&T State University  
**Dr. Esmail Abuhdima**, Benedict College  
**Dr. Pierluigi Pisu**, Clemson University  
**Jian Liu**, University of South Carolina  
**Amirhossein Nazeri**, Clemson University  
**Dr. Abdulmajid A. Mrebit**, Benedict College

## **Contact information**

Chin-Tser Huang, Ph.D.  
550 Assembly Street,  
Columbia, SC 29201  
University of South Carolina  
Phone: (803) 777- 4635; E-mail: [huangct@cse.sc.edu](mailto:huangct@cse.sc.edu)

September 2024



**Center for Connected Multimodal Mobility (C<sup>2</sup>M<sup>2</sup>)**



Benedict College



UNIVERSITY OF  
SOUTH CAROLINA



CLEMSON  
UNIVERSITY

200 Lowry Hall, Clemson University  
Clemson, SC 29634

Center for Connected Multimodal Mobility (C<sup>2</sup>M<sup>2</sup>)  
Clemson University, Benedict College, University of South Carolina

## **DISCLAIMER**

*The contents of this report reflect the views of the authors, who are responsible for the facts and the accuracy of the information presented herein. This document is disseminated in the interest of information exchange. The report is funded, partially or entirely, by the Center for Connected Multimodal Mobility (C<sup>2</sup>M<sup>2</sup>) (Tier 1 University Transportation Center) Grant, which is headquartered at Clemson University, Clemson, South Carolina, USA, from the U.S. Department of Transportation's University Transportation Centers Program. However, the U.S. Government assumes no liability for the contents or use thereof.*

*Non-exclusive rights are retained by the U.S. DOT.*

## ACKNOWLEDGMENT

*This study is partially supported by the Center for Connected Multimodal Mobility (C<sup>2</sup>M<sup>2</sup>) (USDOT Tier 1 University Transportation Center) headquartered at Clemson University, Clemson, SC. Any opinions, findings, and conclusions or recommendations expressed in this paper are those of the authors and do not necessarily reflect the views of C<sup>2</sup>M<sup>2</sup> and the official policy or position of the USDOT/OST-R, or any State or other entity, and the U.S. Government assumes no liability for the contents or use thereof. It is also partially supported by U.S. Department of Energy-National Nuclear Security Administration (NNSA) PuMP, MSIPP IAM-EMPOWEREd, MSIPP, Department of Education MSEIP programs, NASA ULI (University of South Carolina-Lead), and NSF Grant Nos. 1719501, 1954532, and 2131080.*

### Technical Report Documentation Page

<b>1. Report No.</b>	<b>2. Government Accession No.</b>	<b>3. Recipient's Catalog No.</b>	
<b>4. Title and Subtitle</b> Transfer of Technologies for Performance Degradation Prediction and Channel Switching in Vehicular Networks under Harsh Weather Conditions and Integration with State-of-the-Art Products		<b>5. Report Date</b> September 2024	
		<b>6. Performing Organization Code</b>	
<b>7. Author(s)</b> Chin-Tser Huang, Ph.D.; ORCID: 0000-0003-3983-972X Gurcan Comert, Ph.D.; ORCID: 0000-0002-2373-5013 Esmail Abuhdim, Ph.D.; ORCID: 0000-0002-3923-2020 Pierluigi Pisu, Ph.D.; ORCID: 0000-0003-4266-1336 Jian Liu; ORCID: 0000-0001-8368-6228 Amirhossein Nazari; ORCID: 0000-0002-7396-2572 Abdulmajid A. Mrebit, Ph.D.; ORCID: 0000-0002-1696-976X		<b>8. Performing Organization Report No.</b>	
<b>9. Performing Organization Name and Address</b> Computer Science and Engineering Department, University of South Carolina 550 Assembly Street, Columbia, SC 29201		<b>10. Work Unit No.</b>	
		<b>11. Contract or Grant No.</b> 69A3551747117	
<b>12. Sponsoring Agency Name and Address</b> Center for Connected Multimodal Mobility (C <sup>2</sup> M <sup>2</sup> ) USDOT Tier 1 University Transportation Center Clemson University 200 Lowry Hall, Clemson Clemson, SC 29634		<b>13. Type of Report and Period Covered</b> Final Report (10/01/2023 - 09/30/2024)	
		<b>14. Sponsoring Agency Code</b>	
<b>15. Supplementary Notes</b>			
<b>16. Abstract</b> The 5G millimeter wave (mm-Wave) technology has revolutionized modern communication systems with significantly increased data transmission speeds and bandwidth. Despite these advancements, environmental conditions profoundly impact mm-wave signals, particularly in areas prone to dust and sandstorms. These storms, characterized by high concentrations of suspended particles, cause considerable signal attenuation and degradation. This report discusses the development of predictive mathematical models that estimate mm-wave signal degradation under dust and sandstorm conditions. These models incorporate critical factors such as dust particle size distribution, storm intensity, signal frequency, and atmospheric conditions. Addressing the challenges posed by environmental factors, we introduce a Fuzzy Controller for adaptive mm-wave channel switching. This controller leverages advanced algorithms to facilitate smooth and efficient frequency transitions, enhancing signal reliability. Our approach goes beyond conventional solutions that switch between frequencies based solely on signal strength. Instead, it intelligently integrates environmental data, such as visibility and rain intensity, to select optimally from five distinct frequencies, thereby improving the adaptability and effectiveness of 5G networks in adverse weather conditions.			
<b>17. Keywords</b> 5G millimeter wave, sandstorms, signal attenuation, degradation, channel switching, fuzzy controller		<b>18. Distribution Statement</b> No restrictions.	
<b>19. Security Classif. (of this report)</b> Unclassified	<b>20. Security Classif. (of this page)</b> Unclassified	<b>21. No. of Pages</b> 25	<b>22. Price</b> NA

## Table of Contents

DISCLAIMER .....	ii
ACKNOWLEDGMENT .....	iii
LIST OF TABLES .....	vii
LIST OF FIGURES.....	vii
EXECUTIVE SUMMARY.....	1
CHAPTER 1 .....	2
Introduction and Background.....	2
CHAPTER 2 .....	4
Development of Predictive Mathematical Model for Millimeter Wave Degradation in Sandstorm Regions .....	4
2.1 Complex Attenuation factor by Dust and Sand.....	4
2.2 Propagation in Dusty Median .....	6
2.3 Results and Discussion .....	7
2.4 Conclusion .....	11
CHAPTER 3 .....	12
Switching Millimeter Wave Channels Using Fuzzy Controller System.....	12
3.1 Introduction .....	12
3.2 RF Switching Channel.....	13
3.3 System Model .....	14
3.3.1 Rain Attenuation.....	14
3.3.2 Dust and Sand Attenuation .....	14
3.3.3 Free Space Loss Model .....	15
3.4 Fuzzy Control for Frequency Selection Based on Visibility and Rain Conditions .....	15
3.4.1 Fuzzy Logic Model .....	15
3.4.2 Fuzzy Logic Base.....	16
3.4.3 Fuzzy Inference System (FIS).....	17
3.4.4 Equations .....	17
3.5 Simulation and Results .....	17
CHAPTER 4 .....	19
Device Installation.....	19

Transfer of Technologies for Performance Degradation Prediction and Channel Switching in Vehicular Networks under Harsh Weather Conditions and Integration with State-of-the-Art Products

4.1 Cube60 Installation Photos .....	19
4.2 AI Hardware Programming.....	21
4.3 Problem Encountered and Lesson Learned.....	22
CHAPTER 5 .....	23
Conclusions .....	23
REFERENCES.....	24

## LIST OF TABLES

Table 1: Fuzzy Table .....	16
----------------------------	----

## LIST OF FIGURES

Figure 1. A plane wave incident on a spherical sand.....	4
Figure 2. Amplitude of the attenuation factor vs. visibility .....	7
Figure 3. Phase of the attenuation factor vs. visibility .....	8
Figure 4. Amplitude of the attenuation factor vs. particle sand radius .....	9
Figure 5. Phase of the attenuation factor vs. particle sand radius .....	9
Figure 6. Amplitude of the attenuation factor vs. frequency.....	10
Figure 7. Phase of the attenuation factor vs. frequency .....	10
Figure 8. Amplitude of the attenuation factor vs. visibility for Mie and proposed models.....	11
Figure 9. System Block Diagram .....	14
Figure 10. System Output At 4G .....	18
Figure 11. Installation Photos .....	21
Figure 12. NVIDIA Jetson Card .....	21

## EXECUTIVE SUMMARY<sup>1</sup>

In this study, we develop a mathematical model to predict signal degradation in 5G mm-wave communications due to dust and sandstorms. By integrating environmental factors such as particle size and storm intensity, the research enhances the reliability of mm-wave systems in harsh environments, paving the way for robust communications infrastructure. The outcomes improve the robustness of mm-wave technologies and ensure reliability in dust-prone regions, contributing to the advancement of communications infrastructure in challenging conditions.

We also present a fuzzy logic-based system for optimizing 5G mm-wave channel switching, leveraging real-time environmental data to maintain connectivity under adverse conditions. The proposed Fuzzy Controller optimizes channel switching, using real-time environmental data to intelligently select from multiple frequency options, thus maintaining high transmission rates and reducing latency.

In the last part, we integrated the MikroTik Cube 60 devices at Benedict College and highlighted the practical testing of theories presented in the studies. The Cube 60's ability to fail-over to 5GHz in poor weather conditions provides a real-world application of frequency switching that enhances system reliability. Additionally, using NVIDIA Nano AI graphic cards in the studies facilitates the testing of complex computational models and algorithms that drive the adaptive frequency management system, proving crucial for validating the fuzzy logic control approach.

---

<sup>1</sup> Note that the content of this report has been accepted as two conference papers:

One paper will appear in the proceeding of 12th IEEE International Conference on Wireless for Space and Extreme Environments (WiSEE'24) Daytona Beach, FL, USA, December 16-18, 2024. "Development of Predictive Mathematical Model for Millimeter Wave Degradation in Sandstorm Regions".

One paper will appear in the proceeding of IEEE RFID-TA 2024 Daytona Beach, FL, USA, December 18-20, 2024. "Switching Millimeter Wave Channels Using Fuzzy Controller System".



## CHAPTER 1

### Introduction and Background

The propagation of millimeter waves (mm-Waves) through the atmosphere is significantly influenced by environmental factors such as dust and sandstorms. These phenomena, common in arid and semi-arid regions, pose substantial challenges to the reliability and efficiency of mm-wave communication systems. The attenuation and scattering of mm-Waves by dust and sand particles can degrade signal quality, leading to increased error rates and reduced communication range.

Dust and sandstorms are characterized by high airborne particles interacting with electromagnetic waves through scattering and absorption. The extent of these interactions depends on several factors, including the particles' size, shape, and composition, as well as the frequency of the incident wave. Previous studies have shown that mm-Waves' attenuation increases with frequency and particle concentration, making high-frequency bands particularly susceptible to degradation in dusty environments [1]. Understanding these interactions is crucial for designing robust communication systems that operate effectively in such conditions.

The attenuation of mm-Waves in dust and sandstorms can be described using models that account for the scattering and absorption of electromagnetic waves by particles. Mie scattering theory [2], which provides a comprehensive framework for analyzing the interaction of electromagnetic waves with spherical particles, is often employed in these models. According to Mie's theory, particles' scattering, and absorption efficiencies depend on their size relative to the wavelength of the incident wave. Ahmed et al. showed that for mm-waves with wavelengths of 1-10 millimeters, particles with diameters on the order of micrometers to millimeters can cause significant attenuation [3].

In addition to particle size, the incident wave frequency plays a critical role in determining the extent of attenuation. Higher frequencies are generally more susceptible to scattering and absorption, leading to more significant signal degradation [4].

5G technology is widely employed in various applications by offering ultra-fast speeds, low latency, and massive connectivity. It enables transformative applications such as smart cities, autonomous vehicles, remote healthcare, and enhanced mobile broadband. Recently, to address the challenges associated with using 5G mm-Wave in complex weather conditions, Abuhdima et al. [5] explored the effect of dust and sand on the 5G communication channels by using 5G mini links and Mie scattering model to estimate the propagating wave's attenuation [5].

Also, in another work [6], the authors strived to address the impact of harsh weather on the performance and reliability of Connected Vehicles Communication (CVC) through Mie channel modeling. Liu et al. [7] investigated 5G and 4G vehicle-to-vehicle (V2V) communication channel performance under severe weather. Previous research on mm-wave channel performance under harsh weather conditions has overlooked the complex part of the dielectric attenuation coefficient, focusing only on the actual part through Mie scattering modeling. This simplification leads to a significant loss of information in high-frequency channel modeling, resulting in estimation inaccuracies. In this report, we strive to address this problem by introducing complex attenuation related to dust and sand particles and revising the Mie scattering formula to achieve higher channel estimation accuracy.

The remainder of this report is structured into five sections. Chapter 2 explores the development of a predictive mathematical model for millimeter wave degradation in sandstorm-prone regions, while Chapter 3 examines the implementation of a system for switching millimeter wave channels using a fuzzy controller. In Chapter 4, we present various photographs to illustrate our installation of the Cube 60 device at Benedict College in South Carolina and the NVIDIA nano AI graphics card. The final chapter summarizes the report and outlines future plan and recommendations.

## CHAPTER 2

### Development of Predictive Mathematical Model for Millimeter Wave Degradation in Sandstorm Regions

#### 2.1 Complex Attenuation factor by Dust and Sand

The power absorption in the lossy dielectric medium attenuates millimeter waves propagating through dusty regions. The transmitted power is attenuated by the scattering of some energy by the sand particles. In general, the absorption loss is greater than the scattering loss. The attenuation of a spherical sand particle is computed by finding absorption and scattering cross-sections of a single sand. It is considered a spherical sand particle with a radius  $a$ . The sand has a complex dielectric constant  $k' - jk''$  as shown in Fig. 1. The incident electric field is propagating in the direction of x-axes and is defined as [8]:

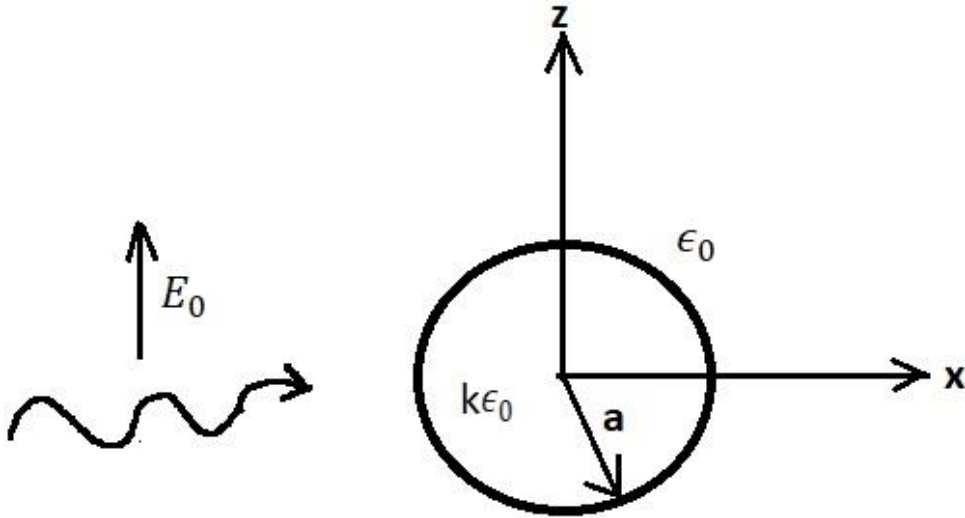


Fig. 1. A plane wave incident on a spherical sand

$$\vec{E}_i = E_0 \hat{a}_z e^{-jk_0 \cdot x} \quad (1)$$

where  $k_0$  is the wave number,  $E_0$  is the amplitude of the incident electric field. First, the absorption cross section is computed by defining the polarization current density in the sphere  $J_p = j\omega P$ . The propagating electrical field related to the polarization current density is

$$\vec{P} = (K - 1) \epsilon_0 E \quad (2)$$

where  $\epsilon_0$  is the permittivity of free space and  $E$  is the incident electrical field. The absorbed average power is written by:

$$P_a = \frac{1}{2} \text{Re} \left[ \iiint_{a, 2\pi, \pi}^{0, 0, 0} E \cdot J_p^* r.^2 \sin \theta \, d\theta, d\phi, dr \right] \quad (3)$$

After the integral is applied, the equation of absorbed average power will be written as:

$$P_a = \frac{2}{3} \pi a^3 \text{Re}[E \cdot Jp^*] \quad (4)$$

The simplified absorbed power as a function in the complex dielectric constant is:

$$P_a = \frac{2}{3} \pi a^3 \epsilon_0 \omega E_0^2 [K'' + j(1 - K')] \quad (5)$$

The absorption across the section is computed by dividing the equation (5) by the incident power density as follows:

$$\sigma_a = \frac{4\pi a^4 \epsilon_0 \omega K_0}{Y_0} [K'' + j(1 - K')] \quad (6)$$

where  $Y_0 = 1/Z_0$  and  $Z_0$  is the characteristic impedance of the free space. The second step is computing the scattered cross section by finding the total scattered power. The far field scattered electrical field can be written as:

$$\vec{E}_s = -\omega Z_0 K_0 P_0 \sin \theta \frac{e^{-jk_0 r}}{4\pi r} a_\theta \quad (7)$$

where  $P_0 = \frac{4}{3} \pi a^2 P$  and  $P = 3 \frac{K-1}{K+2} \epsilon_0 E_0 a_z$ . The total scattered power is written as:

$$P_s = \frac{1}{2} \text{Re} \left[ \iint_{0,0}^{2\pi,\pi} |E_s|^2 r^2 \sin \theta \, d\theta \, d\phi \right] = \frac{\omega^2 K_0^2 Z_0}{12\pi} |P_0|^2 \quad (8)$$

After  $P_0$  is insert into (8), the  $P_s$  is written as:

$$P_s = \frac{1}{2} \omega^2 K_0^2 \epsilon_0^2 E_0^2 a^6 \left| \frac{K-1}{K+2} \right|^2 \quad (9)$$

It is time to compute the scattering cross section  $\sigma_s$  as

$$\sigma_s = \frac{P_s}{P_{in}} = \frac{\omega^2 K_0^2 \epsilon_0^2 a^6}{Y_0} \left| \frac{K-1}{K+2} \right|^2 \quad (10)$$

The total scattered and absorbed cross section  $\sigma_t = \sigma_s + \sigma_a$  is written by adding (6) and (10) as

$$B\sigma_t = \frac{\omega^2 K_0^2 \epsilon_0^2 a^6}{Y_0} \left| \frac{K-1}{K+2} \right|^2 + \frac{4\pi a^4 \epsilon_0 \omega K_0}{Y_0} [K'' + j(1 - K')] \quad (11)$$

The total scattered and absorbed power from the incident wave is calculated by the product of the incident power density per unit area with the total cross section  $\sigma_t$  as following:

$$\sigma_t = \sigma'_t + j\sigma''_t \quad (12)$$

Where  $\sigma'_t = \frac{1}{2}(\omega^2 K_0^2 \varepsilon_0^2 a^6 C_1 + 4\pi a^4 \omega K_0 K'')$  is the real part of the total cross section and  $\sigma''_t = \frac{1}{2}(\omega^2 K_0^2 \varepsilon_0^2 a^6 C_2 + 4\pi a^4 \omega K_0 (1 - K'))$  is the imaginary part of the total cross section.

The constant  $C_1 = \frac{(K'^2 - K''^2 - 2K' + 1)(K'^2 - K''^2 + 2K' + 4) + 4(K'K'' - K'')(K'K'' + K'')}{(K'^2 - K''^2 + 2K' + 4)^2 + 4(K'K'' + K'')^2}$  and  $C_2 = \frac{-2(K'K'' + K'')[4K' + 3]}{(K'^2 - K''^2 + 2K' + 4)^2 + 4(K'K'' + K'')^2}$ . The complex attenuation factor in  $\frac{dB}{Km}$  is given by:

$$A_f = 4.343 \times 10^3 [\sigma'_t + j\sigma''_t] \frac{5.5 \times 10^{-4}}{V a_e} \quad (13)$$

where  $a_e$  is equivalent particle sand radius and  $V = \frac{5.5 \times 10^{-4}}{N a_e^2}$  is the visibility in kilometers (km). The  $N$  is defined *particles/m<sup>3</sup>*. To simplify (13) it is assumed every dust particle is replaced by an equivalent particle  $a_e$  in a real storm [9] and [10].

## 2.2 Propagation in Dusty Median

The propagation of the mm-Wave in a dielectric medium is affected by time delay and losses. This loss could be caused by rain, snow, fog, dust, and sand. The propagation of mm-Wave in the dusty medium is considered herein. The phasor form of the electric field in this dusty region is defined by

$$E = E_0 e^{-A_f} e^{-jk_o \cdot d} \quad (14)$$

The complex attenuation constant ( $\sigma_t$ ) is expressed in Nepers per kilometer by using the following transforming formula [9].

$$A_f \left( \frac{NP}{Km} \right) = \frac{1}{8.68} A_f \left( \frac{db}{Km} \right) \quad (15)$$

The complex attenuation factor in Nepers per kilometer can be written as:

$$A_f = \frac{1}{7.267 V a_e Y_0} [\sigma'_t + j\sigma''_t] \quad (16)$$

The propagating field during dusty medium is computed by

$$E(f) = E_i n(f) e^{-A'_f d} e^{-j(k_o + A''_f) d} \quad (17)$$

where  $E(f)$  is the received field,  $E_i n(f)$  is the transmitted field. The group delay is computed by finding the derivative of the wavenumber at distance  $d$  as [11]:

$$\tau_d(f) = \frac{d}{2\pi} \frac{d\beta}{df} \quad (18)$$

where  $\beta = k_o + A''_f$ .

## 2.3 Results and Discussion

In this section, the MATLAB is used to simulate the proposed model and show the effect of dust and sand on the propagating mm-Wave. The proposed model investigates the effect of dust and sand on the amplitude and the phase of the propagating signal. It is known that the dielectric constant of the transmission medium changes in dusty environments. This change makes the space region a lossy medium instead of lossless medium. The communication channels that use the higher frequency band, such as 5G or 6G, are more affected by these weather factors. In this research, it is considered the dielectric constant of the transmission medium is  $(6.3485-j*0.0929)$  [12, 13]. This value represents the real dielectric constant of dusty regions in the north-Africa desert. Previous research concluded that the humidity has an evident effect on the dielectric constant as represented in the coming two equations [14].

$$\epsilon' = 6.3485 + 0.04H - 7.78 \times 10^{-4}H^2 + 5.56 \times 10^{-6}H^3 \quad (19)$$

$$\epsilon'' = 0.0929 + 0.02H - 3.71 \times 10^{-4}H^2 + 2.76 \times 10^{-6}H^3 \quad (20)$$

According to the real experiment, the average and maximum radius of the particle size are 94.43  $\mu\text{m}$  and 538.04  $\mu\text{m}$ , respectively [15]. The proposed model defined by Equation (13) shows the behavior of propagating mm-Wave during dusty/sandy regions. First of all, the simulation shows the patterns of the amplitude and the phase of the attenuation factor during a change in visibility. It is considered that the radius of a sand particle is 94.43  $\mu\text{m}$ , and the operating frequency is 73 GHz. Fig.2 shows that the attenuation increases when the humidity increases.

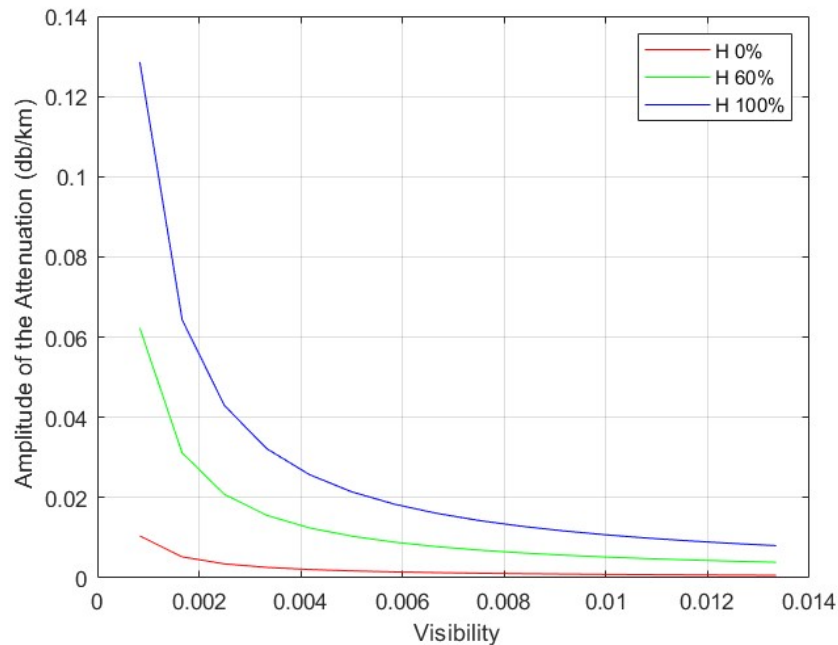


Fig. 2. Amplitude of the attenuation factor vs. visibility

It is shown that the attenuation is  $0.005 \frac{dB}{km}$ ,  $0.031 \frac{dB}{km}$  and  $0.064 \frac{dB}{km}$  when the humidity is 0, 60 and 100 percentage, respectively. It is shown that the phase is changed when the visibility is less than 0.834 m. The phase is constant when the visibility is greater than 0.834 m.

The phase angle is  $-89^\circ$ ,  $-84.8^\circ$  and  $-80.84^\circ$  when the humidity is 0, 60 and 100 percentage respectively in Fig. 3. The effect of particle sand radius on the phase and amplitude of the attenuation factor is investigated.

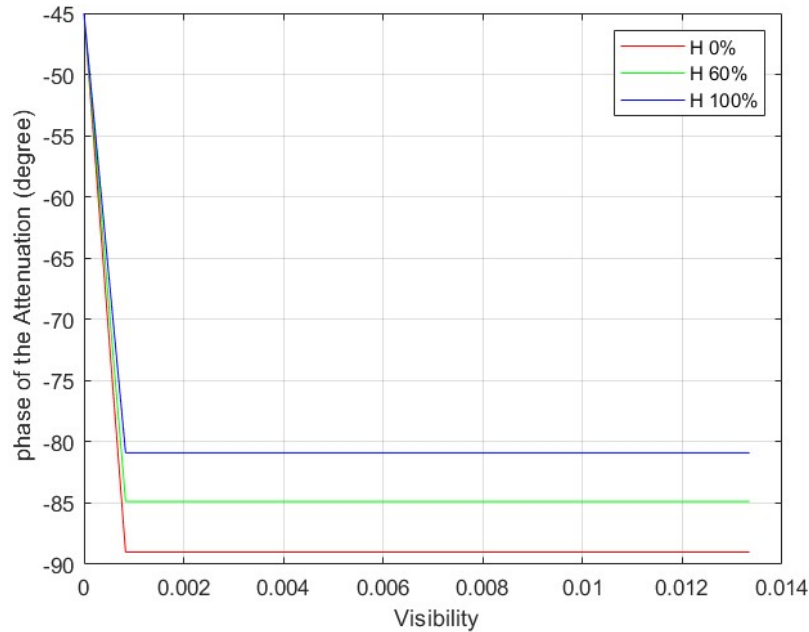


Fig. 3. Phase of the attenuation factor vs. visibility

The visibility is assumed to be 1 m, and the operating frequency is 73 GHz as shown in Fig. 4. The amplitude of the attenuation is increased when the visibility is decreased, and the humidity is increased. The phase shift of the attenuation factor is  $-81^\circ$  in the case of dry weather with 0 percent humidity,  $-85^\circ$  in the case of 60 percent humidity and  $-89^\circ$  in 100 percentage humidity as shown in Fig. 5.

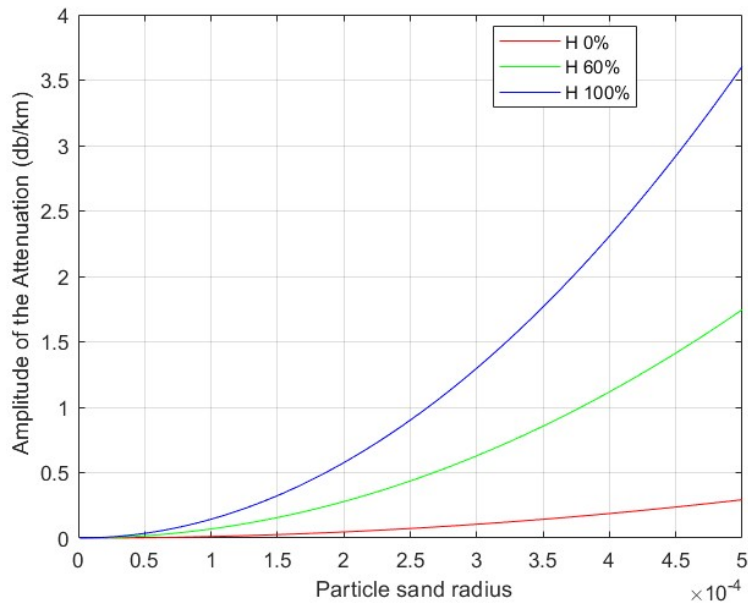


Fig. 4. Amplitude of the attenuation factor vs. particle sand radius

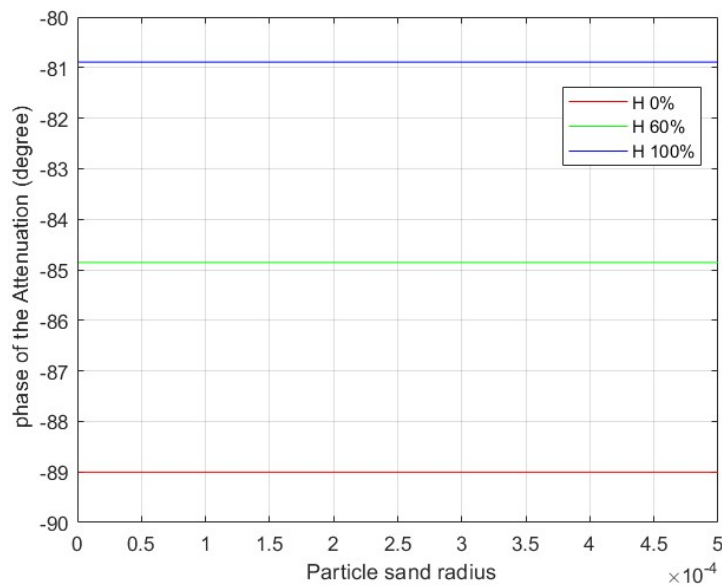


Fig. 5. Phase of the attenuation factor vs. particle sand radius

It is known that the amplitude of the attenuation factor is proportional to the operating frequency. In this simulation, the sand particle radius and the visibility are considered  $94 \mu\text{m}$  and  $1 \text{ m}$ , respectively. Fig. 6 shows that the attenuation is evident when the operating frequency exceeds  $7 \text{ GHz}$ . Also, the attenuation increases proportionally to the operating frequency and humidity.



The phase of attenuation factor is recorded  $-89^\circ$ ,  $-84.85^\circ$  and  $-80.89^\circ$  in the case of 0, 60, and 100 percentage humidity respectively as shown in Fig. 7.

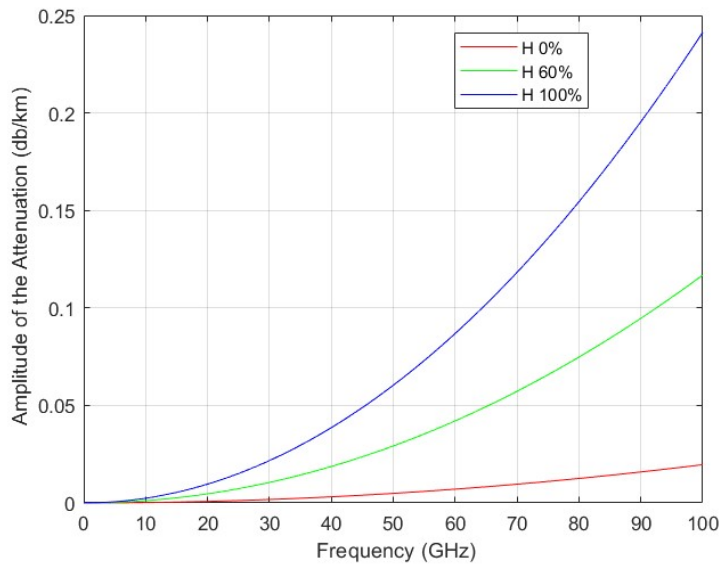


Fig. 6. Amplitude of the attenuation factor vs. frequency

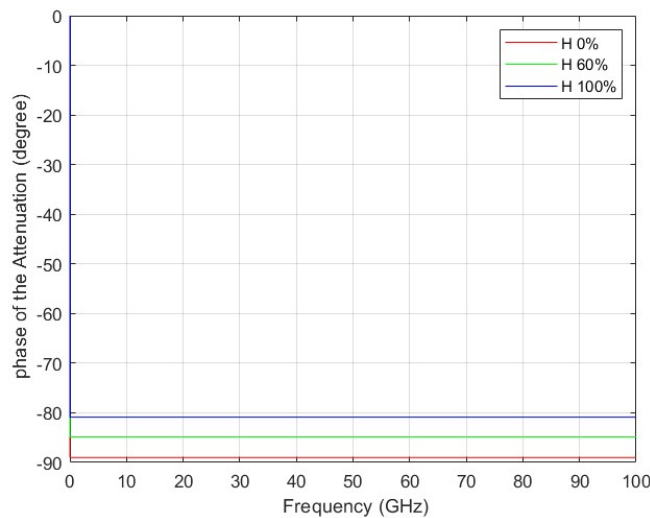


Fig. 7. Phase of the attenuation factor vs. frequency

To this end, the Mie model and new proposed mathematical model that, despite differing in their formulations, yield similar patterns of the amplitude of dust and sand attenuation as shown in Fig.8. The Mie model is not able to represent the effect of dust and sand on the phase of propagating signal in comparison with the new proposed model.

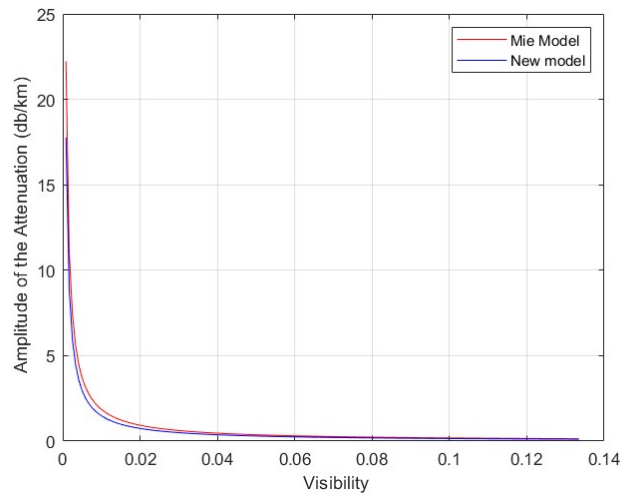


Fig. 8. Amplitude of the attenuation factor vs. visibility for Mie and proposed models

## 2.4 Conclusion

This chapter presents a significant advancement in understanding the impact of dust and sandstorms on millimeter wave (mm-Wave) communication systems through the development of predictive mathematical models. Our proposed model used theoretical principles to accurately investigate the phase and amplitude of the mm-Wave signal due to dusty storms. By incorporating variables such as particle size distribution, storm intensity, and meteorological conditions, the models provide a robust framework for predicting dust and sand's effect on the propagating signal's phase and amplitude.

## CHAPTER 3

### Switching Millimeter Wave Channels Using Fuzzy Controller System

This chapter introduces a novel approach for managing 5G millimeter-wave channel switching, addressing the critical need for high-speed, low-latency communication. While promising significantly higher transmission rates, millimeter-wave frequencies are highly susceptible to environmental conditions such as rain, snow, dust, and sand, leading to signal attenuation and connectivity disruptions. To counter these challenges, we propose a Fuzzy Controller for switching mm-wave channels, which utilizes advanced algorithms to ensure smooth and efficient channel transitions. Our model quantifies the impact of environmental conditions on 5G signal propagation, precisely simulating how rainfall influences signal strength. Unlike devices on the market that typically switch between two frequencies based on signal strength alone, our approach intelligently incorporates environmental data such as visibility and rain intensity to choose optimally from five different frequencies. Through extensive simulations and performance evaluations, we show that our approach ensures reliable connectivity while maintaining high data speeds and minimizing latency. This research sets a foundational platform for future investigations into robust millimeter-wave channel switching mechanisms for 5G networks, enhancing user experience and overall network efficiency.

#### 3.1 Introduction

The rapid advancement of 5G networks has brought forth transformative possibilities for wireless communications, driven by the increasing need for faster data speeds and ultra-low latency. One of the key enablers of these performance improvements is the utilization of millimeter-wave (mm-wave) frequencies; these higher frequencies are crucial for achieving the high data rates promised by 5G [16]. However, deploying mm-wave frequencies poses significant challenges, as these signals are particularly vulnerable to environmental conditions such as rain, snow, dust, and sand, which can lead to severe signal attenuation [7]. This susceptibility undermines the reliability and efficiency of 5G networks, especially in maintaining stable connections during severe weather conditions. Addressing these challenges requires innovative solutions that account for signal propagation and environmental variability to ensure robust communication under adverse conditions.

Current 5G systems primarily switch between a limited set of frequencies, depending predominantly on received signal strength. This method, while functional, often leads to connectivity disruptions under adverse weather conditions and fails to fully leverage the higher throughput potential of millimeter-wave channels like those at 39 GHz and 28 GHz [17]. Furthermore, defaulting to a lower LTE frequency, such as 5 GHz, can significantly degrade transmission rates. The authors in [18] proposed a multi-channel switching strategy, though it lacks an advanced mechanism for channel selection. An improved solution should cover a wider range of frequency channels, enhance network performance, and ensure robust connectivity across varying environmental conditions.

This chapter presents a novel approach, "Switching mm-wave Channels using a Fuzzy Controller," uniquely utilizing five distinct frequency channels to adapt to varying environmental conditions. The fuzzy logic control system intelligently selects the optimal frequency by leveraging real-time visibility and rain intensity measurements to ensure seamless communication. This novel design, incorporating a sophisticated signal attenuation loss model, allows the system to precisely account for severe environmental impacts on mmWave communications, particularly rainfall. Extensive simulations and empirical validations demonstrate that this multi-channel

approach significantly enhances channel reliability, reduces latency, and maintains high data transmission rates, setting a new benchmark for 5G mm-wave technology.

### 3.2 RF Switching Channel

The MikroTik Cube 60 [19] device is a state-of-the-art wireless system that operates in the 60 GHz frequency range, ideal for high-speed point-to-point data transmissions. One of the critical features of the Cube 60 is its ability to automatically fail over to the 5 GHz frequency, providing a reliable backup connection in the event of adverse weather conditions that can significantly impact the 60 GHz signal. This dual-band capability ensures continuous service and enhances the system's resilience, making it an excellent choice for modern network infrastructures that demand high throughput and consistent reliability. However, this fail-over mechanism depends on RSSI (Received Signal Strength Indicator) measurements, which may not proactively respond to changing conditions, often resulting in degraded communication quality before any action is taken. This delayed response can be hazardous in future V2V communication networks, where maintaining seamless connectivity is crucial for safety. There is a crucial need for an advanced system capable of predicting signal degradation before it occurs and providing seamless communication, which is vital in ensuring future vehicle-to-vehicle networks' safety and reliability.

Our proposed module integrates the Cube 60 system with additional real-time weather measurement sensors, enhancing its capability to assess environmental conditions directly. This setup is complemented by a sophisticated interface with MATLAB Simulink, where a detailed block diagram features a fuzzy controller designed for dynamic frequency management. High-precision sensors continuously collect data on rain and visibility, crucial parameters that are processed in real-time and utilized within MATLAB Simulink. The fuzzy controller leverages this up-to-the-minute data to adjust the Cube 60's operating frequency to the most suitable band. This advanced capability ensures efficient and proactive frequency switching, critical for maintaining uninterrupted and safe communication in V2V networks, especially under adverse weather conditions where timely adaptation to signal degradation is vital for safety and reliability.

The system block diagram is shown in Fig. 9. The proposed system consists of a transmitter (modulation), receiver (demodulation), and channel and fuzzy logic control. The wireless channel is modeled using the MATLAB function to compute the Free Space Path Loss (FSPL) for every selected frequency. The proposed fuzzy logic control system provides an efficient and adaptive solution for selecting the optimal communication frequency in response to varying rain and visibility conditions. By utilizing fuzzy rules and membership functions, the system can dynamically adapt to environmental conditions and select the appropriate frequency to ensure reliable communication.

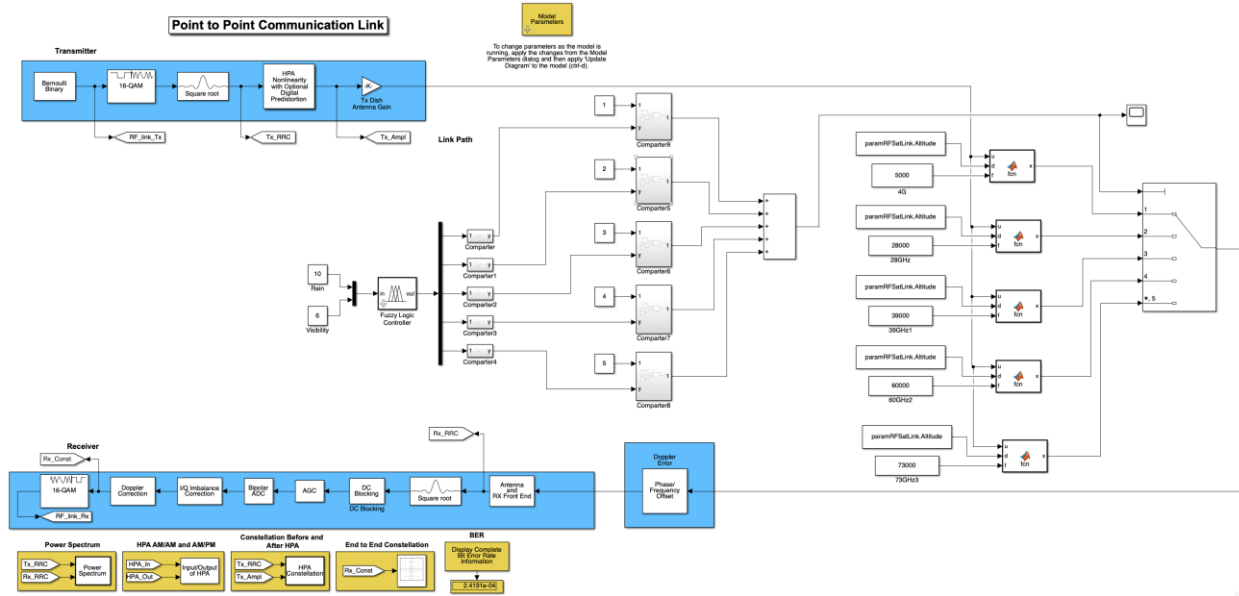


Fig. 9. System Block Diagram

### 3.3 System Model

Free Space Path Loss (FSPL) is essential for understanding the propagation of 5G signals and for designing a switching system that utilizes multi-band transmitters. FSPL describes the attenuation of electromagnetic waves during propagation, significantly impacting coverage and range. By accounting for FSPL, one can optimize link budgets, antenna configurations, and overall system performance. This study enhances the FSPL model by incorporating the effects of environmental factors such as rain, dust, and sand.

#### 3.3.1 Rain Attenuation

Rain attenuation reduces signal strength due to rain interaction with electromagnetic waves. Higher frequencies are more affected. Rain attenuation can be estimated using empirical models:

$$\gamma_R = KR^\alpha \quad (21)$$

where R is the rain rate in *mm/hr*, K and  $\alpha$  depend on frequency, polarization, and elevation.

#### 3.3.2 Dust and Sand Attenuation

Dust and sand particles in the atmosphere can significantly attenuate electromagnetic waves by scattering and absorbing them. This attenuation is particularly relevant in desert regions where sandstorms frequently happen, affecting the reliability and performance of wireless communication. The degree of attenuation can be accurately computed using the Mie scattering model [20]:

$$\alpha_{(dB)} = \frac{a_e f d}{v} [C_1 + C_2 a_e^2 f^2 + C_3 a_e^3 f^3] \quad (22)$$

where  $C_1, C_2, C_3$  depend on the dielectric constant,  $\alpha_e$  is particle diameter,  $v$  is visibility, and  $f$  is frequency.

### 3.3.3 Free Space Loss Model

FSPL quantifies the attenuation of electromagnetic waves as they travel through a clear path. Understanding signal degradation is crucial for wireless communications, especially in free space, where it directly impacts the efficacy and reach of transmission. In urban settings, the updated formula for FSPL, which takes into account rain attenuation and dust/sand attenuation, is given by:

$$FSPL = 38.77 + 16.7 \log f + 18.2 \log d + \alpha + \gamma_R \quad (23)$$

where  $d$  is the distance in km,  $f$  is frequency in GHz, and  $\alpha$  and  $\gamma_R$  are dust/sand and rain attenuation, respectively.

### 3.4 Fuzzy Control for Frequency Selection Based on Visibility and Rain Conditions

In this section, we explore the application of fuzzy control to dynamically choose the optimal communication frequency based on rain intensity and visibility readings from sensors. The system assesses the environmental conditions and selects frequencies from 5 GHz (DSRC), 28 GHz, 39 GHz, 60 GHz, and 73 GHz. This selection process is driven by fuzzy logic rules that account for how rain and visibility affect signal propagation.

#### 3.4.1 Fuzzy Logic Model

Fuzzy logic is a powerful tool for managing uncertainties and non-linearities in environmental conditions. In our system, the primary inputs, Rain Intensity and Visibility, directly influence the output selection of Frequency Band. These inputs are processed using membership functions that quantify the extent to which specific conditions are satisfied.

1) Inputs:

- Rain (R): Rain intensity, measured in inches per hour (in/h), is categorized into discrete ranges significantly influencing signal attenuation.

- $R_1: 0 \leq R \leq 5$  (Low rain)
- $R_2: 5 < R \leq 9$  (Moderate rain)
- $R_3: 9 < R \leq 13$  (Heavy rain)
- $R_4: 13 < R \leq 16$  (Severe rain)
- $R_5: R > 16$  (Very severe rain)

- Visibility (V): Visibility, measured in kilometers, is determined by a sensor and categorized into distinct ranges.

- $V_1: 0 \leq V < 1$  (Very low visibility)
- $V_2: 1 \leq V \leq 5$  (Low visibility)
- $V_3: 5 < V \leq 7$  (Moderate visibility)
- $V_4: 7 < V \leq 10$  (Good visibility)
- $V_5: V > 10$  (Very good visibility)

2) Output: The Frequency Channel(F) to be selected are:

- F<sub>1</sub>: 4G (DSRC)
- F<sub>2</sub>: 5G 28 GHz
- F<sub>3</sub>: 5G 39 GHz
- F<sub>4</sub>: 5G 60 GHz
- F<sub>5</sub>: 5G 73 GHz

### 3.4.2 Fuzzy Logic Base

The selection of the appropriate frequency band in our system is governed by rules that assess two variables: Rain Intensity and Visibility. Each variable is categorized into five distinct value ranges. Consequently, the total number of possible rule combinations in our fuzzy logic system is calculated as  $5^2 = 25$  different rules, allowing for precise adjustments based on the environmental inputs.

Table 1: Fuzzy Table

Fuzzy Rule	Rain Intensity	Visibility	Frequency Channel
1	R <sub>1</sub>	V <sub>1</sub>	F <sub>1</sub>
2	R <sub>1</sub>	V <sub>2</sub>	F <sub>1</sub>
3	R <sub>1</sub>	V <sub>3</sub>	F <sub>2</sub>
4	R <sub>1</sub>	V <sub>4</sub>	F <sub>4</sub>
5	R <sub>1</sub>	V <sub>5</sub>	F <sub>5</sub>
6	R <sub>2</sub>	V <sub>1</sub>	F <sub>1</sub>
7	R <sub>2</sub>	V <sub>2</sub>	F <sub>2</sub>
8	R <sub>2</sub>	V <sub>3</sub>	F <sub>2</sub>
9	R <sub>2</sub>	V <sub>4</sub>	F <sub>4</sub>
10	R <sub>2</sub>	V <sub>5</sub>	F <sub>4</sub>
11	R <sub>3</sub>	V <sub>1</sub>	F <sub>1</sub>
12	R <sub>3</sub>	V <sub>2</sub>	F <sub>1</sub>
13	R <sub>3</sub>	V <sub>3</sub>	F <sub>3</sub>
14	R <sub>3</sub>	V <sub>4</sub>	F <sub>3</sub>
15	R <sub>3</sub>	V <sub>5</sub>	F <sub>4</sub>
16	R <sub>4</sub>	V <sub>1</sub>	F <sub>1</sub>
17	R <sub>4</sub>	V <sub>2</sub>	F <sub>2</sub>
18	R <sub>4</sub>	V <sub>3</sub>	F <sub>2</sub>
19	R <sub>4</sub>	V <sub>4</sub>	F <sub>3</sub>
20	R <sub>4</sub>	V <sub>5</sub>	F <sub>4</sub>
21	R <sub>5</sub>	V <sub>1</sub>	F <sub>1</sub>
22	R <sub>5</sub>	V <sub>2</sub>	F <sub>1</sub>
23	R <sub>5</sub>	V <sub>3</sub>	F <sub>3</sub>
24	R <sub>5</sub>	V <sub>4</sub>	F <sub>1</sub>
25	R <sub>5</sub>	V <sub>5</sub>	F <sub>1</sub>

### 3.4.3 Fuzzy Inference System (FIS)

The decision-making process in a fuzzy logic system consists of the following steps:

- 1) **Fuzzification:** Converts crisp inputs (rain and visibility) into fuzzy values using membership functions.
- 2) **Rule Evaluation:** The fuzzy rules are applied based on the fuzzy values.
- 3) **Aggregation:** The results from each rule are combined to form a fuzzy output.
- 4) **Defuzzification:** Converts the fuzzy output back into a crisp value representing the selected frequency.

### 3.4.4 Equations

The membership functions for Rain and Visibility are represented as follows:

1) Rain Membership Function:

$$\mu_{\text{Rain}}(x) = \begin{cases} 1 & \text{if } 0 \leq x \leq 5 \\ \frac{x-5}{9-5} & \text{if } 5 < x \leq 9 \\ \frac{x-9}{13-9} & \text{if } 9 < x \leq 13 \\ \frac{x-13}{16-13} & \text{if } 13 < x \leq 16 \end{cases}$$

2) Visibility Membership Function:

$$\mu_{\text{Visibility}}(y) = \begin{cases} 1 & \text{if } 0 \leq y \leq 1 \\ \frac{y-5}{5-1} & \text{if } 1 < y \leq 5 \\ \frac{y-5}{7-5} & \text{if } 5 < y \leq 7 \\ \frac{y-7}{10-7} & \text{if } 7 < y \leq 10 \end{cases}$$

These equations describe how the input values are fuzzified based on the rain and visibility conditions, which in turn guide the frequency selection process.

### 3.5 Simulation and Results

The simulation results, illustrated in Fig. 10, depict the received signal across the 5 GHz for 4G, gained from setting the Rain and Visibility inputs to 17 and 1, respectively. Under favorable environmental conditions, the system operates at the highest frequency, 73 GHz. As adverse conditions, such as rain, visibility, and atmospheric disturbances, intensify, the fuzzy controller dynamically switches to lower frequencies. In severe weather, such as heavy rain, the system switches to 4G at 5 GHz. The simulation shows that the selection of radio frequency channel is depended on the values of input rain and visibility sensors. This adaptive mechanism ensures that the received signal strength remains sufficient to maintain uninterrupted communication, preventing signal degradation at the receiver. Using our system by defining weather conditions, we can simulate what frequencies the system would prefer based on the conditions.



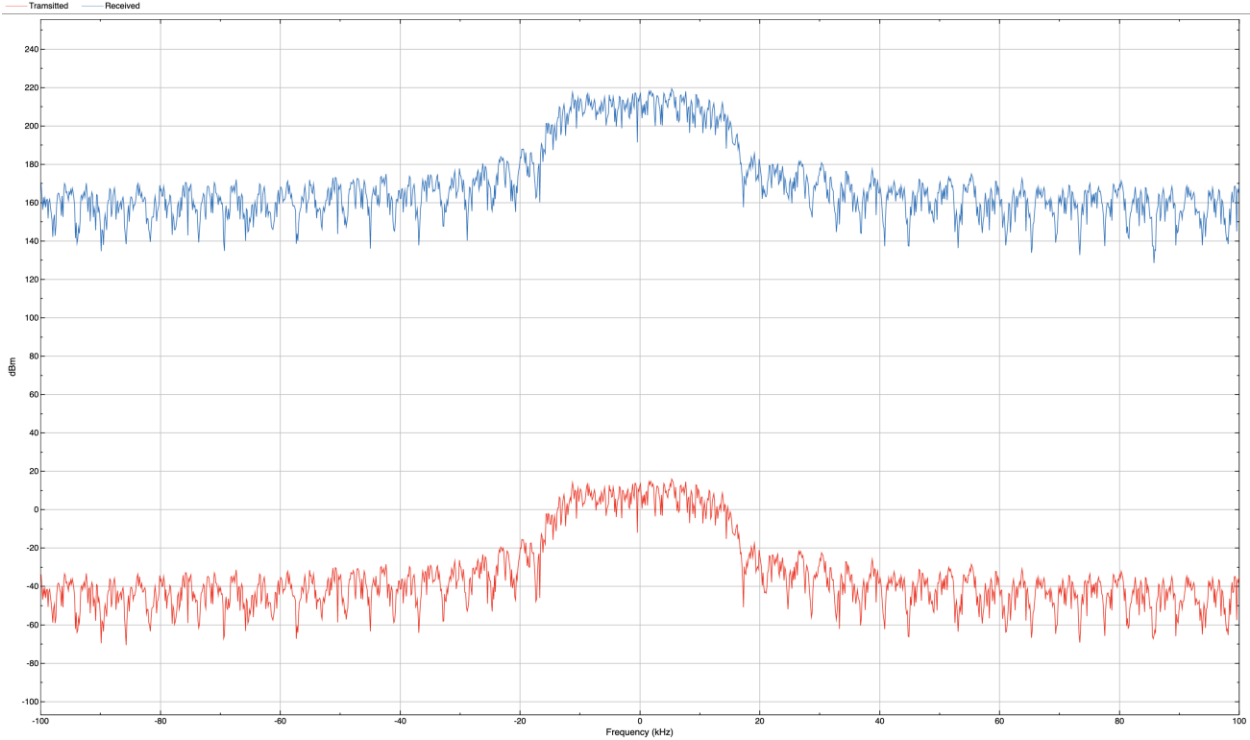


Fig. 10. System Output At 4G

## CHAPTER 4

### Device Installation

As introduced in the summary, a significant component of our project involved the deployment of the Wireless Wire Cube60 Pro at Benedict College in Columbia, South Carolina. Our team dedicated extensive effort to this installation, ensuring that the device was set up efficiently and effectively to meet the specific needs of the college's network infrastructure. This installation not only involved the physical setup of the hardware but also the configuration and testing of the system to ensure optimal performance and reliability.

#### 4.1 Cube60 Installation Photos



Transfer of Technologies for Performance Degradation Prediction and Channel Switching in Vehicular Networks under Harsh Weather Conditions and Integration with State-of-the-Art Products



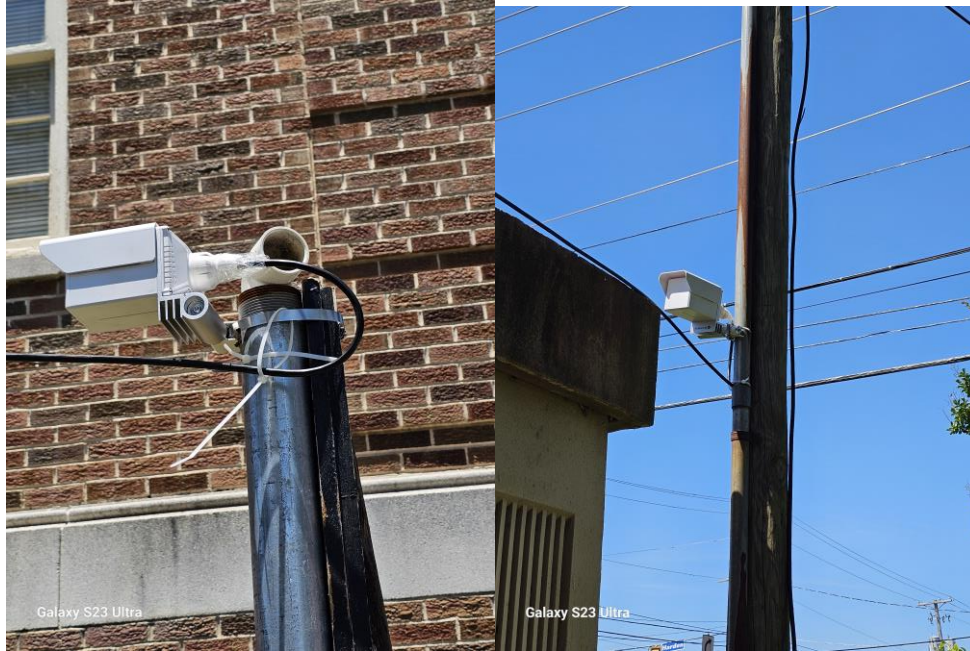


Fig. 11. Installation Photos

#### 4.2 AI Hardware Programming

We allocated an extensive amount of time and effort to implement an end-to-end AI-driven channel switching mechanism through integration of AI-based channel performance estimator with the fuzzy logic-based channel switching decision making and ultimately with Cube60 for experimental validation. In that case, we utilized a NVIDIA Jetson Nano development kit (Fig. 12), a compact powerful AI computing device designed for edge computing and IoT applications, to help perform switching estimation calculations and transfer commands to the device' controller for the physical channel switching.



Fig. 12. NVIDIA Jetson Card

### 4.3 Problem Encountered and Lesson Learned

Our project experienced notable delays due to significant collaboration challenges with MikroTik, a company based in Latvia with limited operational support within the United States. MikroTik's support structure is notably constrained, with only a single representative handling all U.S.-based inquiries. This arrangement has led to considerable communication difficulties, exacerbated by a language barrier and the representative's strong accent. Moreover, there has been a noticeable reluctance on the part of this individual to engage promptly with our emails, which has further impeded our progress.

Efforts to integrate our advanced machine learning techniques with MikroTik's devices were repeatedly hampered by the absence of adequate technical support from their side. Despite multiple attempts to facilitate a productive dialogue, we have yet to achieve successful integration. This lack of support and communication from MikroTik has significantly affected our planned timelines, resulting in delays that impacted the overall advancement of our project.

Despite facing significant challenges during our collaboration with MikroTik, we managed to successfully install the Cube60 device at our campus and conducted tests on rainy days in Columbia, South Carolina. Additionally, we implemented a workaround by using Speedtest [21] as a tool for channel switching. However, this method did not effectively distinguish between 5G mmWave and LTE channels, falling short of our original design objectives. Moving forward, we believe that enhanced collaboration with MikroTik, or potentially exploring similar products from other manufacturers, could lead to the successful development of a new product that meets our specifications.

## CHAPTER 5

### Conclusions

Our first part highlights the importance of considering environmental factors in designing and deploying mm-wave communication systems, particularly in regions prone to dust and sandstorms. The simulation results show that the effect of dust and sand is more evident if the visibility is less than 1m. Also, it is shown that the attenuation by the dust and sand is more evident if the operating frequency is greater than 7 GHz. It offers valuable insights for network engineers and planners, facilitating the development of more resilient communication systems capable of maintaining performance in challenging environments. Future research could extend these models by incorporating additional variables such as particle composition and dynamic storm behavior and exploring real-time adaptation strategies for mm-wave systems.

In the second part, our proposed fuzzy controller effectively controls our proposed channel frequency switching mechanism, which leverages real-time sensor inputs to enhance system robustness. Our system ensures that the received signal strength remains sufficient to maintain uninterrupted communication at the receiver side. This dynamic approach ensures more reliable 5G mmWave communication by adapting to weather changes such as rain or sandstorms. Our simulation results confirm that fuzzy control in channel switching maintains communication integrity and optimizes performance, making it a superior choice for managing the complexities of real-world wireless communication environments.

In summary, the predictive models developed in this study represent a crucial step toward enhancing the reliability of mm-wave communications in dust and sandstorm regions, paving the way for more effective and resilient wireless networks in these challenging conditions. We plan to develop a more granular approach to frequency selection that involves machine learning techniques to predict and respond to changes in weather conditions more accurately and quickly.

## REFERENCES

- [1] Zilberman, A., and Kopeika, N. (2022). A Simple Model for Assessing Millimeter-Wave Attenuation in Brownout Conditions Sensors, 22(22),8889.
- [2] Al-Saman, Ahmed M. et al. "Statistical Analysis of Rain at Millimeter Waves in Tropical Area." IEEE Access 8 (2020): 51044-51061.
- [3] Ahmed, A. (1987). Role of particle-size distributions on millimeter-wave propagation in sand/dust storms in Proceedings H Microwaves, Antennas and Propagation.
- [4] E. M. Abuhdima and I. M. Saleh, "Effect of sand and dust storms on microwave propagation signals in southern Libya," Melecon 2010 – 2010 15th IEEE Mediterranean Electrotechnical Conference, 2010, pp. 695-698, doi: 10.1109/MELCON.2010.5475995.
- [5] E. M. M. Abuhdima et al., "The effect of Dust and Sand on the 5G Millimeter-Wave links," 2021 IEEE International Conference on Wireless for Space and Extreme Environments (WiSEE), 2021, pp. 60-65, doi: 10.1109/WiSEE50203.2021.9613843.
- [6] E. Abuhdima et al., "Impact of Dust and Sand on 5G Communications for Connected Vehicles Applications," in IEEE Journal of Radio Frequency Identification, vol. 6, pp. 229-239, 2022, doi: 10.1109/JRFID.2022.3161391.
- [7] J. Liu et al., "Investigation of 5G and 4G V2V Communication Channel Performance Under Severe Weather," 2022 IEEE International Conference on Wireless for Space and Extreme Environments (WiSEE), Winnipeg, MB, Canada, 2022, pp. 12-17, doi: 10.1109/WiSEE49342.2022.9926867
- [8] Collin R., E., Antenna and radiowave propagation (McGraw-hill International Edition, Singapore, 1985).
- [9] Z. Elabdin, M. R. Islam, O. O. Khalifa, H. E. A. Raouf and M. J. E. Salami, "Development of mathematical model for the prediction of microwave signal attenuation due to dust storm," 2008 International Conference on Computer and Communication Engineering, Kuala Lumpur, Malaysia, 2008, pp. 1156-1161, doi: 10.1109/ICCCE.2008.4580788.
- [10] Constantine A. Balanis, Advanced Engineering Electromagnetics. Wiley,2012.
- [11] Golovachev, Y.; Etinger, A.; Pinhasi, G.A.; Pinhasi, Y. Millimeter Wave High Resolution Radar Accuracy in Fog Conditions—Theory and Experimental Verification. Sensors 2018, 18, 2148. <https://doi.org/10.3390/s18072148>.
- [12] E. M. Abuhdima and I. M. Saleh, "Effect of sand and dust storms on GSM coverage signal in southern Libya," 2010 International Conference on Electronic Devices, Systems and Applications, 2010, pp. 264-268, doi: 10.1109/ICEDSA.2010.5503063.
- [13] E. M. Abuhdima and I. M. Saleh, "Effect of sand and dust storms on microwave propagation signals in southern Libya," Melecon 2010 – 2010 15th IEEE Mediterranean Electrotechnical Conference, 2010, pp. 695-698, doi: 10.1109/MELCON.2010.5475995.
- [14] E. M. Abuhdima and I. M. Saleh, "Effect of sand and dust storms on GSM coverage signal in southern Libya," 2010 International Conference on Electronic Devices, Systems and Applications, 2010, pp. 264-268, doi: 10.1109/ICEDSA.2010.5503063
- [15] I. M. Saleh, H. M. Abufares and H. M. Snousi, "Estimation of wave attenuation due to dust and sandstorms in southern Libya using Mie model," WAMICON 2012 IEEE Wireless and Microwave Technology Conference, 2012, pp. 1-5, doi: 10.1109/WAMICON.2012.6208467.
- [16] S. A. Busari, S. Mumtaz, S. Al-Rubaye, and J. Rodriguez, "5G Millimeter-Wave Mobile Broadband: Performance and Challenges," IEEE Communications Magazine, vol. 56, no. 6, pp. 137–143, Jun. 2018.
- [17] W.-Y. Li, W. Chung, and J.-H. Chou, "Highly Integrated Wideband 28 GHz and 39 GHz Array Antennas for 5G Mobile Phone Applications," in 2020 IEEE International Symposium on Antennas and Propagation and North American Radio Science Meeting. Montreal

[18] J. Liu, A. Nazeri, C. Zhao, E. Abuhdima, G. Comert, C.-T. Huang, and P. Pisu, "Switching Strategy for Connected Vehicles Under Variant Harsh Weather Conditions," *IEEE Journal of Radio Frequency Identification*, vol. 7, pp. 371–378, 2023

[19] "Wireless Wire Cube Pro | MikroTik." [Online]. Available: [https://mikrotik.com/product/wireless wire cube pro](https://mikrotik.com/product/wireless_wire_cube_pro)

[20] S. M. Sharif, "ATTENUATION PROPERTIES OF DUSTY MEDIA USING MIE SCATTERING SOLUTION," *Progress in Electromagnetics Research M*, vol. 43, pp. 9–18, 2015.

[21] "librespeed/speedtest." LibreSpeed, Dec. 10, 2024. Available: <https://github.com/librespeed/speedtest>. [Accessed: Dec. 09, 2024]